

On the efficient preconditioning of the Stokes equations in tight geometries.

Vladislav Pimanov¹, Oleg Iliev¹, Ivan Oseledets^{2,3}, and Ekaterina Muravleva²

¹Fraunhofer ITWM, Kaiserslautern, Germany

²Skolkovo Institute of Technology, Moscow, Russia

³Artificial Intelligence Research Institute, Moscow, Russia

Emails: vladislav.pimanov@itwm.fraunhofer.de,
oleg.iliev@itwm.fraunhofer.de, i.oseledets@skoltech.ru,
e.muravleva@skoltech.ru

July 12, 2023

Abstract

If the Stokes equations are properly discretized, it is well-known that the Schur complement matrix is spectrally equivalent to the identity matrix. Moreover, in the case of simple geometries, it is often observed that most of its eigenvalues are equal to one. These facts form the basis for the famous Uzawa and Krylov-Uzawa algorithms. However, in the case of complex geometries, the Schur complement matrix can become arbitrarily ill-conditioned having a significant portion of non-unit eigenvalues, which makes the established Uzawa preconditioner inefficient. In this article, we study the Schur complement formulation for the staggered finite-difference discretization of the Stokes problem in 3D CT images and synthetic 2D geometries. We numerically investigate the performance of the CG iterative method with the Uzawa and SIMPLE preconditioners and draw several conclusions. First, we show that in the case of low porosity, CG with the SIMPLE preconditioner converges faster to the discrete pressure and provides a more accurate calculation of sample permeability. Second, we show that an increase in the surface-to-volume ratio leads to an increase in the condition number of the Schur complement matrix, while the dependence is inverse for the Schur complement matrix preconditioned with the SIMPLE. As an explanation, we conjecture that the no-slip boundary conditions are the reason for non-unit eigenvalues of the Schur complement.

Keywords: Stokes problem, tight geometry, preconditioned Krylov subspace methods

1 Introduction

The steady-state flow of a slow incompressible fluid in the domain Ω is governed by the Stokes equations:

$$\begin{aligned} -\Delta \mathbf{u} + \nabla p &= \mathbf{f}, \text{ in } \Omega \\ -\nabla \cdot \mathbf{u} &= 0, \text{ in } \Omega \\ &+ \text{b.c. on } \partial\Omega, \end{aligned} \tag{1}$$

equipped with proper boundary conditions on $\partial\Omega$ (see Section 2.2 for the boundary conditions considered in this paper). Here p denotes the fluid pressure, \mathbf{u} is the fluid velocity, and \mathbf{f} is the source. The discretization of the BVP (1) leads to a block system of linear equations of the following form:

$$\mathbb{A} \begin{bmatrix} \mathbf{u}_h \\ p_h \end{bmatrix} = \begin{bmatrix} \mathbf{f}_h \\ g_h \end{bmatrix}, \quad \mathbb{A} = \begin{bmatrix} \mathbf{A} & \mathbf{B}^T \\ \mathbf{B} & \end{bmatrix}, \tag{2}$$

where \mathbf{A} and \mathbf{B} are discrete counterparts of the negative velocity Laplacian operator and the negative divergence operator which, under proper discretization is an adjoint of the discrete pressure gradient operator \mathbf{B}^T . The boundary conditions are incorporated in the discretization matrices.

We consider the Pressure Schur Complement formulation (according to the terminology from [23]) which reduces the system (2) to the following equivalent equation on the discretized pressure:

$$Sp_h = g_h^S, \tag{3}$$

where S is the Schur complement of the $(0,0)$ -th block of the matrix \mathbb{A} and g_h^S is the right-hand-side in the reduced equation, which are defined as follows:

$$S = \mathbf{B}\mathbf{A}^{-1}\mathbf{B}^T, \quad g_h^S = \mathbf{B}\mathbf{A}^{-1}\mathbf{f}_h - g_h. \tag{4}$$

Once the pressure is computed, the velocity can be recovered by solving the following equation:

$$\mathbf{A}\mathbf{u}_h = \mathbf{f}_h - \mathbf{B}^T p_h. \tag{5}$$

If the Stokes equations (1) are properly discretized such that the discrete operators preserve important properties of the continuous ones, then (up to a constant in its nullspace) the Schur complement matrix S is known to be spectrally equivalent to the identity operator acting on the discrete pressure space. For example, in the context of the finite element method, the equivalence to the pressure mass matrix takes place with the right choice of LBB-stable elements (see e.g. [24]), and in the context of the finite difference discretization, this equivalence can be observed for mimetic discretization of the divergence and gradient operators, see, e.g., [13]. For earlier introduction of the mimetic approach see, e.g., [22].

In particular, spectral equivalence to the identity means that the condition number of S does not increase under the mesh refinement process. Moreover, it

is often observed that most of the eigenvalues of S are equal to one. In fact, when solving the boundary value problem (1), the spectrum of S strongly depends on the boundary conditions imposed. The most common boundary conditions for the Stokes flow on solid walls are the no-slip boundary conditions, and this is due to the presence of the no-slip boundaries the spectrum of the Schur complement contains eigenvalues which are not equal to one. When one solves problems with small surface-to-volume ratio, which is the case most commonly considered in papers analyzing iterative solvers for Stokes problems, only a small part of eigenvalues of the Schur complement are not equal to one, which justifies using a diagonal matrix or even the identity matrix as a preconditioner. These facts are the basis for the Uzawa and Uzawa-like algorithms [4, 8, 6, 23, 9, 1], which are classical algorithms for solving the steady Stokes problem (1).

Note, that Uzawa algorithm can be written in two equivalent formulations (see, e.g., [4] p.44). In the first one, as a stationary iteration for the coupled system (2) preconditioned with a block triangular preconditioner (see, e.g., [5, 4]), while in the second one, the Uzawa algorithm is written as an iterative method for the Schur complement equation (3) (see, e.g., [1, 23]). Numerous computational studies, using either of the formulations, demonstrate the efficiency of the Uzawa algorithms in the case of simple geometries. A number of reviews and theoretical studies are dedicated to this subject advancing the knowledge in the area, see, e.g. [4, 17, 16]. Even a superlinear convergence of the Krylov-Uzawa algorithm can be established for general smooth geometries, see [1]. On the other hand, the Schur complement matrix S can become arbitrarily ill-conditioned for very complex geometries, like ones representing the pore space in rock samples, filter media, membranes, etc.. In particular, we demonstrate the later issue in Section 4.1, where we present specific rock samples from tight reservoirs for which the condition number of S is greater than 10^5 .

Recently, it was demonstrated in [15] that adding discrete diffusion to the established preconditioner significantly reduces the number of iterations in the case of channel-dominated domains. Similar results were demonstrated in [20] for the diffusion-like SIMPLE preconditioner in the case of complex geometries from tight porous media.

The SIMPLE and the Uzawa preconditioners for the Schur complement S , \hat{S}_{simple} and \hat{S}_{uzawa} , can be written as follows:

$$\hat{S}_{simple} = \mathbf{B}\hat{\mathbf{A}}_{simple}^{-1}\mathbf{B}^T, \quad \hat{\mathbf{A}}_{simple} = \text{diag}(\mathbf{A}), \quad \hat{S}_{uzawa} = I. \quad (6)$$

In fact, the preconditioner \hat{S}_{simple} is widely-known in the CFD community since the same approximation is used in the SIMPLE iterative method (Semi-Implicit Method for Pressure Linked Equations), which is one of the classical methods for solving the stationary Navier-Stokes equations [19]. It should be noted, that in the Stokes case, the spectrum of \hat{S}_{simple} is qualitatively different from the spectrum of S . Namely, the matrix \hat{S}_{simple} behaves essentially as the pressure Laplacian matrix $\mathbf{B}\mathbf{B}^T$, so its condition number increases quadratically as the grid resolution decreases. However, such spectral behavior turns out to be justified in the case of tight geometries in the presence of narrow channels where

the nature of flow is predominantly diffusive.

In the present article, we numerically investigate the behavior of the two preconditioners for the staggered finite-difference discretization of Stokes equations describing the flow in tight rock samples and in synthetic 2D geometries, and identify certain domain characteristics which are indicators for the performance of the respective Stokes solvers.

The remainder of the paper is organized as follows. Next section is dedicated to the problem statement. The description of the considered iterative methods, namely the CG-Uzawa and CG-SIMPLE methods, is provided in the third section. The main results are presented in the fourth section where the computational experiments are performed and can be summarized as follows.

- In Section 4.1, we compare the CG-SIMPLE and CG-Uzawa algorithms for 3D samples from real rocks with low porosity and confirm by the numerical experiments that the preconditioner \hat{S}_{simple} provides orders of magnitude lower condition numbers than \hat{S}_{uzawa} and demonstrates robust convergence while the CG-Uzawa method stagnates. Further on, we show that the CG-SIMPLE algorithm calculates the permeability much more accurately, which means it calculates the pressure gradient more accurately.
- We show that there is a correlation between the condition number of the Schur complement matrix and the surface-to-volume ratio of the samples. In Section 4.2, we perform a systematic study for the synthetic 2D geometries - random packings of squares, which demonstrates a clear dependence between the condition number of both unpreconditioned and preconditioned with the SIMPLE Schur complement matrices and the surface-to-volume ratio. The results are valid for 3D samples as well (see Section 4.1).
- Further on, we compute the full spectra of the Schur complement matrix and observe that the number of its non-unit eigenvalues is determined by the surface area of the boundary where the no-slip conditions are posed, and by the connectivity of the flow domain.

Finally, conclusions are drawn.

2 Problem statement

The considered here Stokes problem is presented in the Introduction, along with the general algebraic form of its discretization. In this section, the way of representing the geometries, the grid, and the boundary conditions are discussed.

2.1 Voxel-based geometries

In voxel-based geometry, the domain is discretized into small cubic volumes called voxels. For the three-dimensional case, let the computational domain Ω

be a cube with side length L , and let it be decomposed into n^3 voxels, where n is the number of voxels in each dimension:

$$\bar{\Omega} = \bigcup_{(i,j,k) \in \mathbb{I}^n} \omega(i,j,k), \quad \mathbb{I}^n = (i,j,k) : i,j,k \in 1, \dots, n, \quad (7)$$

where \mathbb{I}^n denotes a three-dimensional index set. The voxels $\omega(i,j,k)$ are defined as cubic regions of length $h = L/n$:

$$\omega(i,j,k) = [x_{i-1}, x_i] \times [y_{j-1}, y_j] \times [z_{k-1}, z_k], \quad (8)$$

where $x_i = (i-1)h$, $y_j = (j-1)h$, and $z_k = (k-1)h$.

Each voxel can either represent fluid or solid material. The domain Ω is partitioned into two disjoint parts, the pure fluid domain Ω_f and the solid domain Ω_s :

$$\bar{\Omega} = \bar{\Omega}_f \cup \bar{\Omega}_s. \quad (9)$$

which corresponds to disjoint decomposition:

$$\mathbb{I}^n = \mathbb{I}_f^n \cup \mathbb{I}_s^n. \quad (10)$$

Example of voxel-based geometry for the case $d = 2$ can be seen in Fig. 4, and several samples for the case $d = 3$ are shown in Fig. 1. The classical finite difference method is used to discretize the Stokes problem in Ω_f on fully-staggered grids. The described voxel-based geometry serves as a grid for the pressure, the momentum equations are discretized on staggered grids. For detailed description see, e.g., [12, 11, 14].

2.2 Boundary conditions

Recall, in the fluid domain $\Omega_f = \Omega \setminus \bar{\Omega}_s$, we consider the Stokes equations:

$$\begin{aligned} -\Delta \mathbf{u} + \nabla p &= \mathbf{f} \quad \text{in } \Omega_f, \\ -\nabla \cdot \mathbf{u} &= 0 \quad \text{in } \Omega_f, \\ \mathbf{u} &= \mathbf{0} \quad \text{on } \Gamma_0. \end{aligned} \quad (11)$$

No-slip boundary conditions are imposed on the interior solid boundary Γ_0 , defined as follows:

$$\Gamma_0 = \bar{\Omega}_f \cap \bar{\Omega}_s. \quad (12)$$

Periodic boundary conditions on the velocity and pressure are imposed on the outer boundaries of the computational domain:

$$\begin{aligned} \mathbf{u}|_{\Gamma_x^0 \cap \bar{\Omega}_f} &= \mathbf{u}|_{\Gamma_x^1 \cap \bar{\Omega}_f}, \quad \mathbf{u}|_{\Gamma_y^0 \cap \bar{\Omega}_f} = \mathbf{u}|_{\Gamma_y^1 \cap \bar{\Omega}_f}, \\ p|_{\Gamma_x^0 \cap \bar{\Omega}_f} &= p|_{\Gamma_x^1 \cap \bar{\Omega}_f}, \quad p|_{\Gamma_y^0 \cap \bar{\Omega}_f} = p|_{\Gamma_y^1 \cap \bar{\Omega}_f}, \end{aligned} \quad (13)$$

where $\Gamma_x^0 = \{(x,y) \in \partial\Omega \mid x = 0\}$, and $\Gamma_x^1, \Gamma_y^0, \Gamma_y^1$ are defined similarly. In the case of periodic boundary conditions, the periodicity of the geometry is usually also assumed. It should be noted, that the Stokes problem (11)-(13) is well-posed if and only if the fluid domain Ω_f is connected and $\int_{\Omega_f} p \partial\omega = 0$.

3 Iterative methods under consideration

A variety of methods for solving (2) can be roughly divided into two categories: coupled methods, in which the system is solved in the full form, and reduced methods, in which one of the variables is first excluded from the equations and then restored. In what follows, we consider the (reduced) preconditioned Schur complement equation (3), which can be written as follows:

$$\hat{S}^{-1}Sp_h = \hat{S}^{-1}g_h^S, \quad (14)$$

with the preconditioners either $\hat{S} = \hat{S}_{uzawa}$ or $\hat{S} = \hat{S}_{simple}$ defined in (6).

As it was previously mentioned, the classical SIMPLE and Uzawa algorithms can be equivalently written as stationary iterations in either coupled or reduced form. For the coupled form, usually the GMRES Krylov subspace method is used to accelerate stationary iterations (see, e.g., [2, 16]). Following [1], we use here the Conjugate Gradient (CG) method as the Krylov accelerator for solving the Schur complement problem (14). In fact, different Krylov accelerators of the SIMPLE or Uzawa algorithms may result in non-equivalent iterative methods. In the present section we describe the respective CG-SIMPLE and CG-Uzawa algorithms.

3.1 Description of the methods

A wide class of preconditioners for the stationary Stokes equations (see, e.g., [4, 16, 2, 3, 7]), including the classical SIMPLE and Uzawa algorithms in their coupled forms, can be constructed by discarding one or more factors in the following approximation of the matrix \mathbb{A} :

$$\hat{\mathbb{A}} = \hat{\mathbb{L}}\hat{\mathbb{D}}\hat{\mathbb{U}} = \begin{bmatrix} \mathbf{I} & \\ \mathbf{B}\hat{\mathbf{A}}_1^{-1} & I \end{bmatrix} \begin{bmatrix} \hat{\mathbf{A}}_2 & \\ & -\hat{S} \end{bmatrix} \begin{bmatrix} \mathbf{I} & \hat{\mathbf{A}}_3^{-1}\mathbf{B}^T \\ & I \end{bmatrix}, \quad (15)$$

where $\hat{\mathbf{A}}_1$, $\hat{\mathbf{A}}_2$, $\hat{\mathbf{A}}_3$ are (possibly different) approximations of \mathbf{A} , and \hat{S} is an approximation of S . Popular options are block lower triangular, block diagonal, and block upper triangular preconditioners:

$$\hat{\mathbb{L}}\hat{\mathbb{D}} = \begin{bmatrix} \hat{\mathbf{A}} & \\ \mathbf{B} & -\hat{S} \end{bmatrix}, \quad \hat{\mathbb{D}} = \begin{bmatrix} \hat{\mathbf{A}} & \\ & -\hat{S} \end{bmatrix}, \quad \hat{\mathbb{D}}\hat{\mathbb{U}} = \begin{bmatrix} \hat{\mathbf{A}} & \mathbf{B}^T \\ & -\hat{S} \end{bmatrix}, \quad (16)$$

where $\hat{\mathbf{A}}$ is an approximations of \mathbf{A} . Let us consider a stationary iteration corresponding to the operator splitting $\mathbb{A} = \hat{\mathbb{A}} - (\hat{\mathbb{A}} - \mathbb{A})$, given as follows:

$$\begin{bmatrix} \mathbf{u}_h^{k+1} \\ p_h^{k+1} \end{bmatrix} = \begin{bmatrix} \mathbf{u}_h^k \\ p_h^k \end{bmatrix} + \hat{\mathbb{A}}^{-1} \left(\begin{bmatrix} \mathbf{f}_h \\ g_h \end{bmatrix} - \mathbb{A} \begin{bmatrix} \mathbf{u}_h^k \\ p_h^k \end{bmatrix} \right). \quad (17)$$

For certain choices of the preconditioner $\hat{\mathbb{A}}$ (see below), the coupled iterations (17) can be equivalently rewritten as a preconditioned Richardson iteration for the reduced system (14):

$$p_h^{k+1} = p_h^k + \alpha \hat{S}^{-1}(g_h^S - Sp_h^k), \quad (18)$$

where $\alpha > 0$ is a stationary parameter of the Richardson iteration.

3.1.1 Uzawa and CG-Uzawa algorithms

Let us consider the classical Uzawa algorithm in the following form (see., e.g., [4]):

$$\begin{cases} \mathbf{A}\mathbf{u}_h^{k+1} = \mathbf{f}_h - \mathbf{B}^T p_h^k, \\ \hat{S}_{uzawa} \delta p_h^k = \alpha_{uzawa} (\mathbf{B}\mathbf{u}_h^{k+1} - g_h), \\ p_h^{k+1} = p_h^k + \delta p_h^k, \end{cases} \quad (19)$$

where α_{uzawa} is a relaxation parameter of the algorithm. Firstly, as it is shown in [10], the Uzawa iteration (19) can be regarded as a stationary iteration of the form (17) with a preconditioner $\hat{\mathbf{A}}$ given as follows:

$$\hat{\mathbf{A}} = \hat{\mathbf{A}}_{uzawa} = \begin{bmatrix} \mathbf{A} & \\ \mathbf{B} & -(1/\alpha_{uzawa})\hat{S}_{uzawa} \end{bmatrix}, \quad (20)$$

which corresponds to the block lower triangular preconditioner $\hat{\mathbf{L}}\hat{\mathbf{D}}$ defined in (16) if we take:

$$\hat{S} = (1/\alpha_{uzawa})\hat{S}_{uzawa}, \quad \hat{\mathbf{A}} = \mathbf{A}. \quad (21)$$

Secondly, the Uzawa iteration (19) is equivalent to the Richardson iteration (18) (see, e.g. [4]), if we take:

$$\hat{S} = \hat{S}_{uzawa}, \quad \alpha = \alpha_{uzawa}. \quad (22)$$

The CG-Uzawa algorithm is obtained by replacing the stationary iteration (18) by the Conjugate Gradient iteration applied to \hat{S} with the identity preconditioner \hat{S}_{uzawa} , see, e.g., [1] for details.

3.1.2 SIMPLE and CG-SIMPLE algorithms

Let us now consider the classical SIMPLE algorithm in the following form [19, 7]:

$$\begin{cases} \mathbf{A}\mathbf{u}_h^{k+\frac{1}{2}} = \mathbf{f}_h - \mathbf{B}^T p_h^k, \\ \hat{S}_{simple} \delta p_h^k = \alpha_{simple} (\mathbf{B}\mathbf{u}_h^{k+\frac{1}{2}} - g_h), \\ \hat{\mathbf{A}}_{simple} \delta \mathbf{u}_h^k = -\mathbf{B}^T \delta p_h^k, \\ p_h^{k+1} = p_h^k + \delta p_h^k, \\ \mathbf{u}_h^{k+1} = \mathbf{u}_h^{k+\frac{1}{2}} + \delta \mathbf{u}_h^k, \end{cases} \quad (23)$$

where α_{simple} is a pressure damping parameter of the algorithm and \hat{S}_{simple} is defined in (6). Firstly, as it is shown in [7], the iterative process (23) can be regarded as a coupled iteration of the form (17) with the preconditioner $\hat{\mathbf{A}}$ given as follows:

$$\hat{\mathbf{A}} = \hat{\mathbf{A}}_{simple} = \begin{bmatrix} \mathbf{A} & \\ \mathbf{B} & -(1/\alpha_{simple})\hat{S}_{simple} \end{bmatrix} \begin{bmatrix} \mathbf{I} & \hat{\mathbf{A}}_{simple}^{-1} \mathbf{B}^T \\ & I \end{bmatrix}, \quad (24)$$

which corresponds to a preconditioner $\hat{\mathbb{A}}$ of the block structure (15) if we take:

$$\hat{\mathbf{A}}_1 = \hat{\mathbf{A}}_2 = \hat{\mathbf{A}}, \quad \hat{\mathbf{A}}_3 = \hat{\mathbf{A}}_{simple}, \quad \hat{S} = (1/\alpha_{simple})\hat{S}_{simple}. \quad (25)$$

Secondly, the SIMPLE iteration (23) is equivalent to the Richardson iteration (18) (see, e.g. [23]), if we take:

$$\hat{S} = \hat{S}_{simple}, \quad \alpha = \alpha_{simple}. \quad (26)$$

Similarly to the CG-Uzawa algorithm, the CG-SIMPLE algorithm is defined by applying the Preconditioned Conjugate Gradient method to S with the preconditioner \hat{S}_{simple} .

It should be noted, that different splittings of \mathbb{A} in the coupled iterations (17) may result in the same reduced iteration (18). For example, replacing \hat{S}_{uzawa} , α_{uzawa} by \hat{S}_{simple} , α_{simple} in (20) results in the following preconditioner $\hat{\mathbb{A}}$:

$$\hat{\mathbb{A}} = \hat{\mathbb{A}}_{simple}^* := \begin{bmatrix} \mathbf{A} & \\ \mathbf{B} & -(1/\alpha_{simple})\hat{S}_{simple} \end{bmatrix}, \quad (27)$$

which corresponds to the block lower triangular preconditioner $\mathbb{L}\mathbb{D}$ defined in (16) if we take:

$$\hat{S} = (1/\alpha_{simple})\hat{S}_{simple}, \quad \hat{\mathbf{A}} = \mathbf{A}. \quad (28)$$

Then, the coupled iteration (17) with the preconditioner $\hat{\mathbb{A}} = \hat{\mathbb{A}}_{simple}^*$ determines the following iterative process:

$$\begin{cases} \mathbf{A}u_h^{k+1} = \mathbf{f}_h - \mathbf{B}^T p_h^k, \\ \hat{S}_{simple} \delta p_h^k = \alpha_{simple} (\mathbf{B}u_h^{k+1} - g_h), \\ p_h^{k+1} = p_h^k + \delta p_h^k, \end{cases} \quad (29)$$

which can be regarded as the preconditioned (with \hat{S}_{simple}) Uzawa algorithm. In the same time, the iterative process (29) is also equivalent to the Richardson iteration (18) for the choice (26), hence it is also equivalent to the classical SIMPLE algorithm (23). So, following the terminology from [6, 8], the CG-SIMPLE algorithm can be also identified as the preconditioned CG-accelerated Uzawa algorithm.

3.2 Inner iterations and stopping criteria

For both the CG-Uzawa and CG-SIMPLE algorithms, in our numerical experiments we use unpreconditioned relative residual norm as a stopping criteria for the outer iterative process. Namely, given an input tolerance ε_S , the outer CG iterations stop as soon as:

$$\|r_S^\# \| / \|r_S^0\| < \varepsilon_S, \quad (30)$$

where the superscript $\#$ denotes the final iteration number, and r_S^k denotes the residual on the k^{th} outer iteration, given as follows:

$$r_S^k = Sp_h^k - g_h^S. \quad (31)$$

On each step of the outer iteration, applying matrix S requires inversion of the velocity Laplacian matrix \mathbf{A} to recover intermediate velocity from the intermediate pressure. We use the Preconditioned Conjugate Gradient for solving with the velocity Laplacian matrix \mathbf{A} , so formally we deal with inexact versions [6, 8] of the Uzawa and SIMPLE algorithms. Thus, we have a two-level inner-outer iterative process: at each step of the outer CG iteration for S , inner CG iterations for \mathbf{A} are performed. In our numerical experiments, we use preconditioned relative residual norm as the stopping criteria for inner iterations with matrix \mathbf{A} . For example, given an input tolerance $\varepsilon_{\mathbf{A}}$, the inner CG iteration for computing $\mathbf{u}_h = \mathbf{A}^{-1}\mathbf{f}^h$ stops as soon as:

$$\|(\hat{\mathbf{A}})^{-1}r_{\mathbf{A}}^{\#}\|/\|(\hat{\mathbf{A}})^{-1}r_{\mathbf{A}}^0\| < \varepsilon_{\mathbf{A}}, \quad (32)$$

where $r_{\mathbf{A}}^k$ denotes the residual on the k^{th} inner iteration, given as follows:

$$r_{\mathbf{A}}^k = \mathbf{A}\mathbf{u}_h^k - \mathbf{f}_h. \quad (33)$$

Additionally, at each step of the outer CG-SIMPLE iteration, we have to solve the system with the preconditioner matrix \hat{S}_{simple} . We use preconditioned relative residual norm as the stopping criteria for inner iterations with the matrix \hat{S}_{simple} . For example, given an input tolerance $\varepsilon_{\hat{S}}$, the inner CG iteration for computing $p_h = (\hat{S}_{simple})^{-1}g^h$ stops as soon as

$$\|(\hat{S}_{simple})^{-1}r_{\hat{S}}^{\#}\|/\|(\hat{S}_{simple})^{-1}r_{\hat{S}}^0\| < \varepsilon_{\hat{S}}, \quad (34)$$

where $r_{\hat{S}}^k$ denotes the residual on the k^{th} inner iteration, given as follows:

$$r_{\hat{S}}^k = (\hat{S}_{simple})p_h^k - g_h. \quad (35)$$

For building preconditioners $\hat{\mathbf{A}}$ and \hat{S}_{simple} for the Laplacian matrices \mathbf{A} and \hat{S}_{simple} , we use Algebraic Multigrid method (AMG) [21]. In practice, we use the implementation BoomerAMG [27] from HYPRE library. It is also worth mentioning recent advances in developing monolithic AMG methods for the Stokes problem [25].

4 Computational experiments

Computational experiments are performed in order to study numerically:

- The performance of the two preconditioners in solving the Schur complement problem (3);
- The performance of the two preconditioners in computing the permeability of the samples according to (40);
- Possible correlation between the surface-to-volume ratio and the condition number of the preconditioned/unpreconditioned Schur complement matrix;

- Possible correlation between the number of boundary nodes where the no-slip boundary conditions are imposed and the number of non-unit eigenvalues of the Schur complement matrix.

Two sets of experiments are performed.

In the first one, 3D CT images of samples of rocks from tight reservoirs (low porosity) are considered. The performance of the inexact Uzawa and SIMPLE preconditioners in conjunction with the conjugate gradient method for the Schur complement matrix is compared. It is observed that the SIMPLE preconditioner behaves much better for this class of problems. A correlation between the surface-to-volume ratio and the condition number of the Schur complement matrix is observed. Furthermore, the permeabilities computed with the two preconditioners are compared, and it is shown that the usage of the CG-SIMPLE leads to a much more robust and accurate calculation of the permeability. This implies that the SIMPLE preconditioner not only ensures more robust convergence in solving the Schur complement problem with respect to the pressure, but also provides a more accurate computation of the gradient of the pressure. In the second set of computational experiments, a more rigorous study of the two preconditioners is conducted by considering the synthetic 2D geometries and the exact inner iterations. In addition to comparing the performance of the preconditioners, a systematic study of the spectra of the Schur complement matrix is carried out, and a conjecture that the no-slip boundary conditions are the main reason for the non-unit eigenvalues of the Schur complement is formulated. Moreover, for the considered synthetic samples, we clearly observe that an increase in the surface-to-volume ratio leads to an increase in the condition number of the Schur complement matrix, while the dependence is inverse for the Schur complement matrix preconditioned with the SIMPLE.

4.1 3D rock samples from tight reservoirs

4.1.1 Preliminaries: samples and notations

In this section, we study the performance of the CG-Uzawa and CG-SIMPLE algorithms for the pore space images of real rock samples from tight reservoirs. We consider six 3D images: five ultra-tight samples $A - E$ considered in the article [18], and one image of the classical Berea's sandstone with medium porosity. The corresponding pore space images are depicted on Fig. 1 using the Geodict visualization tool. The samples $A - E$ are scanned with the resolution 1.2 mkm and have the size $n = 600$, and the sample S is scanned with the resolution 4 mkm and has the size $n = 300$. Detailed information about the samples can be found in Table 1, which includes the reference permeability $\bar{\kappa}_{zz}^{\text{ref}}$ defined in (40), the number of fluid voxels $V^f = |\mathbb{I}_f^n|$, and the porosity ν , defined as follow:

$$\nu = (V^f / V) \cdot 100\%, \quad (36)$$

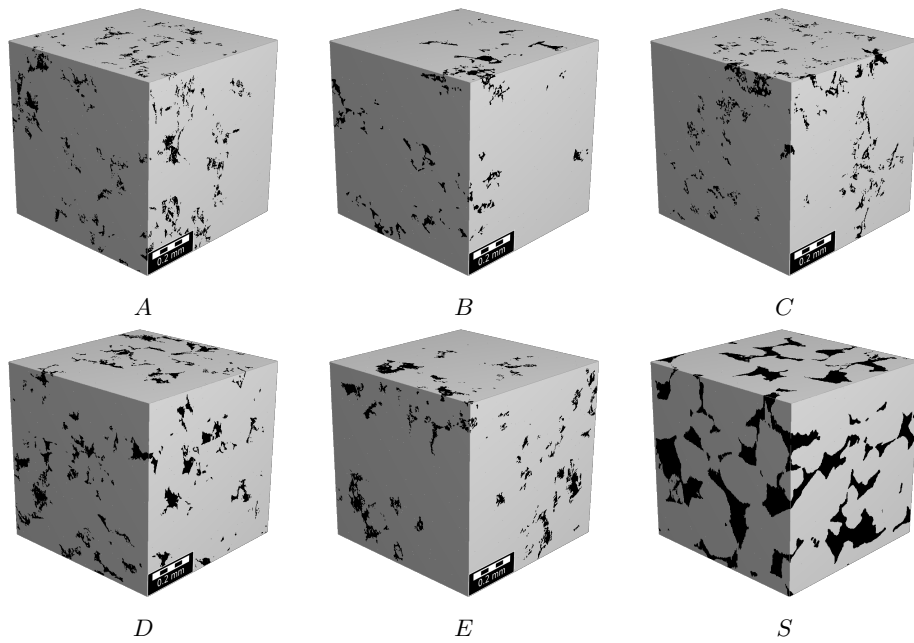


Figure 1: Pore space images of real rock samples: $A - E$ are ultra-tight images from [18], and S is a moderate porosity image of the Berea's sandstone. See Table 1 for more details.

where $\mathbb{V} = |\mathbb{I}^n| = n^d$ is the total number of voxels. Additionally, for each sample we compute the surface-to-volume (s-t-v) ratio which is defined as follows:

$$\sigma_s = (\mathbb{V}_{surf}^s / \mathbb{V}^f) \cdot 100\%, \quad (37)$$

where the surface area \mathbb{V}_{surf}^s of the no-slip boundary is determined as the number of near-boundary solid voxels, i.e., solid voxels face-adjacent with the fluid domain:

$$\mathbb{V}_{surf}^s = |\mathbb{I}_{surf}^n|, \quad \mathbb{I}_{surf}^n = \{(i, j, k) \in \mathbb{I}_s^n : \omega_{(i,j,k)} \cap \bar{\Omega}_f \neq \emptyset\}. \quad (38)$$

Computing permeability. Computing permeability of 3D CT images of rocks or of synthetic 2D geometries is a basic task in the Digital Rock Physics. To compute permeability of a sample in x direction, we solve the Stokes equations with the forcing term $\mathbf{f} = (1, 0, 0)^T$. For Ω having a unit length, such a unit volume force corresponds to a unit pressure drop [26], so in this case permeability equals the Darcy (averaged) velocity, which is given as follows:

$$(\kappa_{xx}, \kappa_{xy}, \kappa_{xz})^T = (\langle u \rangle, \langle v \rangle, \langle w \rangle)^T = \langle \mathbf{u} \rangle = |\Omega|^{-1} \int_{\Omega_f} \mathbf{u}. \quad (39)$$

Note, in order to compute permeabilities in y and z directions, similar computations are required with $\mathbf{f} = (0, 1, 0)^T$ and $\mathbf{f} = (0, 0, 1)^T$. For non-unit domains, the non-dimensional permeability κ_{xx} is scaled by the size of the physical domain in the flow direction:

$$\bar{\kappa}_{xx} = L^2 \kappa_{xx}. \quad (40)$$

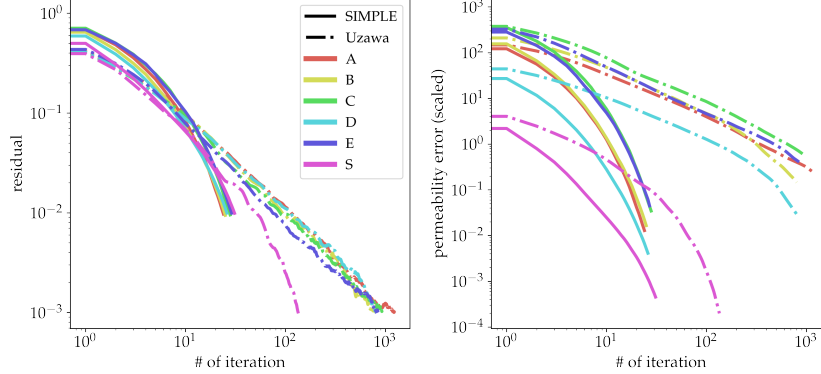
Table 1: Description of 3D samples $A - S$ including the problem size n , reference permeabilities $\bar{\kappa}_{zz}^{\text{ref}}$, the number of fluid voxels \mathbb{V}^f , the porosity ν , and the surface-to-volume ratio σ_s .

	A	B	C	D	E	S
size n	600	600	600	600	600	300
perm. $\bar{\kappa}_{zz}^{\text{ref}}$, mD	0.65	0.78	0.31	9.6	0.75	$6.61 \cdot 10^3$
# pores \mathbb{V}^f , mln.	12.5	9.4	11.4	20.9	13.9	5.7
porosity ν , %	5.8	4.4	5.3	9.7	6.4	21.1
s-t-v ratio σ_s , %	74	56	70	55	61	28

4.1.2 Performance of the preconditioners in solving the Schur complement problem and in computing the permeability

In the present subsection, we study the performance of the SIMPLE and Uzawa preconditioners in solving the Schur complement problem (3) as well as in computing the permeability for the samples $A - S$ described in Table 1. As a stopping criteria for the outer CG iterations, we use $\varepsilon_S = 10^{-3}$ for the CG-Uzawa algorithm and $\varepsilon_S = 10^{-2}$ for the CG-SIMPLE algorithm. It is worth

Figure 2: Convergence history of the CG-SIMPLE and CG-Uzawa algorithms for 3D samples $A - S$ described in the Table 1. Unpreconditioned relative residual norm $\|r_S^k\|/\|r_S^0\|$ (left) and scaled permeability error e_κ^k (right) are shown.



noting that such a smaller stopping tolerance for the CG-Uzawa was used in an attempt, albeit unsuccessful, to achieve convergence in permeability to its reference values κ_{zz}^{ref} . For the inner iterations, we use a higher precision $\varepsilon_{\mathbf{A}} = 10^{-5}$ in both cases. Also, for the CG-SIMPLE algorithm we use $\varepsilon_{\hat{S}} = 10^{-5}$ for solving with the SIMPLE preconditioner \hat{S}_{simple} . The reference permeabilities were computed using the CG-SIMPLE algorithm with higher precision $\varepsilon_S = 10^{-4}$, $\varepsilon_{\mathbf{A}} = 10^{-7}$, $\varepsilon_{\hat{S}} = 10^{-7}$. Such inexact solves for \mathbf{A} and \hat{S}_{simple} make it difficult to rigorously analyze underlying numerical methods. However, the purpose of this section is to demonstrate convergence problems with the established Uzawa preconditioner that occur in practical permeability calculations when computing flows in tight porous media. So, we compare methods for the settings that we usually use in our practical calculations.

The convergence history for selected tolerances is presented in Fig. 2, where the relative unpreconditioned residual norm $\|r_S^k\|/\|r_S^0\|$ defined in (31) is shown on the left. Furthermore, the scaled permeability error, defined as:

$$e_\kappa^k = |\kappa_{zz}^k / \kappa_{zz}^{\text{ref}} - 1|, \quad (41)$$

is shown in Fig. 2 on the right. Recall, that the permeability is computed according to (40), and the velocity is computed according to (5). Having in mind that the left hand side of (5) is identical for both the Uzawa and SIMPLE preconditioned algorithms, the difference in the accuracy with which the permeability is computed can be explained only by the difference in the accuracy with which $\mathbf{B}^T p$ is computed in both cases. Recall that in [20] the computation of the permeability with the current CG-SIMPLE algorithm was compared to computations with other commercial and academic codes, and it was shown that all the values are in the same range.

The summary of the results with CG-Uzawa and CG-SIMPLE algorithms for the 3D real rock samples $A - S$ can be found in Table 2, which includes the num-

ber of iterations, the required computational time, and the scaled permeability error $e_{\kappa}^{\#}$ computed on the final iteration. Additionally, we provide estimations for the condition numbers of the preconditioned and unpreconditioned Schur complement matrices, computed for free during the outer CG iterations using Lanczos algorithm.

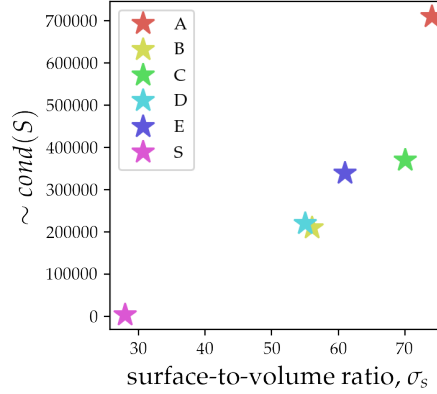
Table 2: Summary of the results for CG-Uzawa and CG-SIMPLE algorithms for 3D samples $A - S$ described in the Table 1 including the scaled permeability error on the final iteration $e_{\kappa}^{\#}$, the total computational time, the number of iterations, and the condition numbers.

	A	B	C	D	E	S
CG-Uzawa:						
perm. error $e_{\kappa}^{\#}$, %	0.221	0.146	0.585	0.029	0.403	0.0002
total comp. time, hrs	8.5	5.0	6.2	10.9	7.3	0.8
# iters	1238	802	946	809	849	136
$\approx \text{cond}(S)$	$7.1 \cdot 10^5$	$2.1 \cdot 10^5$	$3.7 \cdot 10^5$	$2.2 \cdot 10^5$	$3.4 \cdot 10^5$	$3.4 \cdot 10^3$
CG-SIMPLE:						
perm. error $e_{\kappa}^{\#}$, %	0.013	0.016	0.034	0.004	0.044	0.0005
total comp. time, hrs	0.3	0.3	0.3	0.7	0.5	0.3
# iters	25	26	29	27	30	31
$\approx \text{cond}(\hat{S}_{\text{simple}}^{-1} S)$	$0.9 \cdot 10^2$	$1.2 \cdot 10^2$	$1.4 \cdot 10^2$	$1.1 \cdot 10^2$	$1.8 \cdot 10^2$	$2.4 \cdot 10^2$

The following hardware was used in our numerical experiments: 48x MPI compute node (Dell PowerEdge M640), dual Intel Xeon Gold 6132 ("Skylake") @ 2.6 GHz, i.e. 28 CPU cores per node. The computational times shown in Table 2 were obtained using 8 CPU nodes.

Several observations can be drawn from the results presented in Table 2. For the considered low porosity images, the SIMPLE preconditioner appears to perform better than the Uzawa preconditioner, as it converges robustly while the CG-Uzawa stagnates. Firstly, despite the CG-SIMPLE algorithm being more expensive (approximately x1.5) per iteration, its total computational time is smaller compared to the CG-Uzawa because significantly fewer number of iterations is required. This observation holds true for low porosity samples with high surface-to-volume ratios, whereas for higher porosity, the CG-Uzawa shows better performance. Secondly, the estimated condition number for the preconditioned Schur complement matrix is about three orders of magnitude smaller for the SIMPLE preconditioner than for the Uzawa (identity) preconditioner in the case of low porosity. For moderate porosity (sample S), the condition number for both preconditioners is comparable. Thirdly, the CG-SIMPLE computes the permeability much more accurately for the considered samples. As mentioned earlier, this means that it calculates the pressure gradient more accurately for such problems. Actually, achieving even 10% accuracy in computing permeability is not always possible with the CG-Uzawa method.

Figure 3: Correlation between surface-to-volume ratio and estimated condition number for the samples $A - S$ described in the Table 1.



4.1.3 Correlation between the surface-to-volume ratio and the condition number of the Schur complement matrix

In Fig. 3, we show that for the considered samples $A - S$ there is a strong correlation between the surface-to-volume ratio σ_s (37) and the estimated condition number of the unpreconditioned Schur complement matrix. However, the dependence in the case of SIMPLE preconditioned Schur complement matrix is not so distinctive here, so we perform a more rigorous study in the subsequent Section 4.2.3.

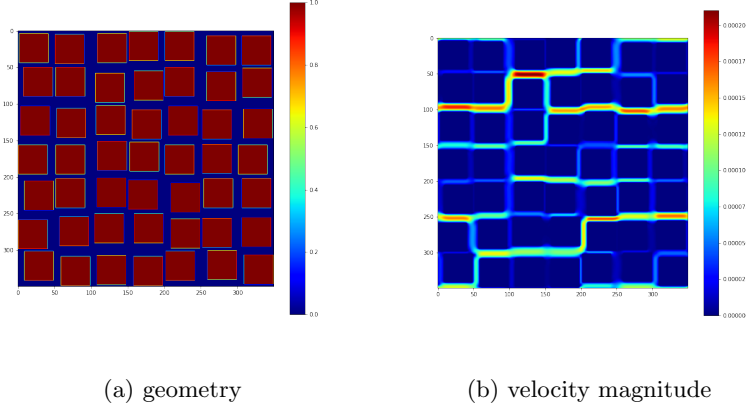
4.2 Two-dimensional synthetic geometries

To identify consistent patterns that affect the performance of the methods under consideration in complex pore space domains, we consider synthetic 2D geometries with a transparent generation process and directly available geometric information (such as porosity, no-slip surface area, etc). As in the 3D case, we present and discuss the convergence of the two algorithms, as well as the accuracy with which the permeability is computed. Additionally, for the considered synthetic samples we compute and analyse the full spectra of the preconditioned and unpreconditioned Schur complement matrices.

4.2.1 Generation of synthetic 2D geometries.

We study flows passing around arrays of solid square obstacles randomly placed in a fluid bed. First of all, a uniform voxel (pixel in 2D) grid is generated in Ω as described in Section 2. For ease of generation, we consider square obstacles of the same size, and each obstacle is located in the center of the square cell, or is slightly shifted, so that a cell contains the obstacle and a part of the flow domain

Figure 4: Example of synthetic 2D geometry: array of randomly shifted square obstacles for $N = 7$, $n_s = 40$, $n_{\text{avg}} = 10$, $n_{\text{min}} = 2$.

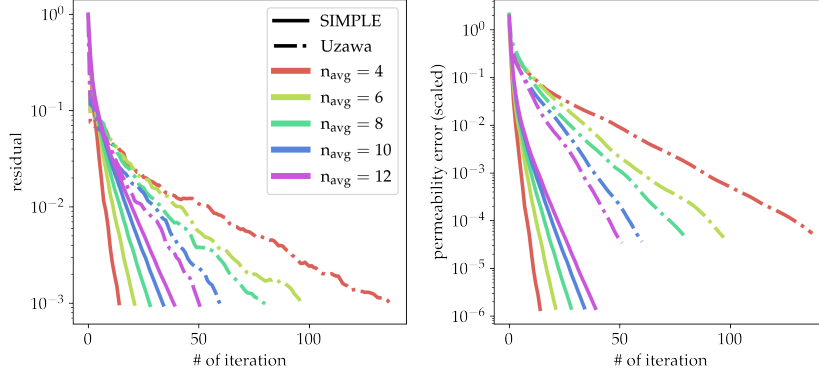


around it. The obstacles do not touch the boundary of the cell. Each generated geometry is defined by four integer parameters $(N, n_c, n_{\text{avg}}, n_{\text{min}})$, where N and n_c determine the number of cells in one direction and their size measured in voxels, while the parameters n_{avg} and n_{min} control the average and minimal thicknesses (in voxels) of the fluid channels between two adjacent solid squares. Note, that the cells and the obstacles in all cases are adjusted to the introduced computational grid, so that each voxel is fully occupied either by fluid or by solid. An example for $N = 7$, $n_c = 50$, $n_{\text{avg}} = 10$, $n_{\text{min}} = 2$ is presented in Fig. 4a. Formally, we have a domain of the total size $n \times n$, $n = Nn_c$ which represents an $N \times N$ array of cells of the size $n_c \times n_c$; each cell contains a solid square of the size $(n_c - n_{\text{avg}}) \times (n_c - n_{\text{avg}})$ with the origin $(n_c/2 + r_1, n_c/2 + r_2)$, where $r_1, r_2 \in [-(n_{\text{avg}} - n_{\text{min}})/2, (n_{\text{avg}} - n_{\text{min}})/2]$ are (integer) random shifts. It should be noted, that randomness is necessary to observe non-trivial solutions which take place in the case of fully periodic arrays.

4.2.2 Performance of the preconditioners in solving the Schur complement problem and in computing permeability

In the present subsection, we study the performance of the SIMPLE and Uzawa preconditioners in solving the Schur complement problem (3) as well as in computing the permeability for the synthetic 2D geometries with variable average channel thicknesses n_{avg} . Namely, we randomly generated five geometries according to the procedure described in the previous subsection for $N = 7$, $n_c = 50$, $n_{\text{min}} = 2$, and $n_{\text{avg}} = \{4, 6, 8, 10, 12\}$. Detailed information about the samples can be found in Table 3, which includes the reference permeability κ_{zz}^{ref} defined in (39), the number of fluid voxels \mathbb{V}^f , the porosity ν (36), and the surface-to-volume (s-t-v) ratio σ_s (37). It should be noted, that the aver-

Figure 5: Convergence history of the CG-SIMPLE and CG-Uzawa algorithms for the synthetic 2D geometries with variable channel thicknesses n_{avg} described in the Table 3. Unpreconditioned relative residual norm $\|r_S^k\|/\|r_S^0\|$ (right) and scaled permeability error e_κ^k (left) are shown.



age channel thickness for synthetic 2D geometries is straightforwardly related to the surface-to-volume ratio for general porous media. Therefore, by varying the average thickness of the synthetic geometries, we can investigate the effect of surface-to-volume ratio on the convergence of the algorithms.

Table 3: Description of the synthetic 2D geometries with variable channel thicknesses n_{avg} including the problem size n , reference permeabilities κ_{xx}^{ref} , the number of fluid voxels \mathbb{V}^f , the porosity ν , and the surface-to-volume ratio σ_s .

	$n_{\text{avg}} = 4$	$n_{\text{avg}} = 6$	$n_{\text{avg}} = 8$	$n_{\text{avg}} = 10$	$n_{\text{avg}} = 12$
size n	350	350	350	350	350
perm. κ_{xx}^{ref}	$1.01 \cdot 10^{-6}$	$3.17 \cdot 10^{-6}$	$7.31 \cdot 10^{-6}$	$1.50 \cdot 10^{-5}$	$2.53 \cdot 10^{-5}$
# pores \mathbb{V}^f , thsnd.	18.8	27.6	36.0	44.1	51.8
porosity ν , %	15.4	22.6	29.4	36.0	42.3
s-t-v ratio σ_s , %	46.9	30.5	22.3	17.3	14.0

As a stopping criteria for the outer CG iterations, we use $\varepsilon_S = 10^{-3}$ for both preconditioners. However, in this experiment we use machine epsilon $\varepsilon_{\mathbf{A}} = \varepsilon_{\hat{S}} = 10^{-13}$ for inner iterations, which means that exact Uzawa is used here. The convergence history for selected tolerances is presented in Fig. 5, where the relative unpreconditioned residual norm $\|r_S^k\|/\|r_S^0\|$ defined in (31) is shown on the left and the scaled permeability error e_κ^k defined in (41) is shown on the right.

The summary of the results obtained with CG-Uzawa and CG-SIMPLE algorithms for the synthetic 2D geometries with variable channel thicknesses can be found in Table 4, which includes the number of iterations, the required computational time, the scaled permeability error $e_\kappa^\#$ computed on the final iteration,

and the condition numbers of the preconditioned and unpreconditioned Schur complement matrices.

Table 4: Convergence summary of the CG-Uzawa and CG-SIMPLE algorithms for the synthetic 2D geometries with variable channel thicknesses n_{avg} described in the Table 3 including the scaled permeability error on the final iteration $e_{\kappa}^{\#}$, the total computational time, the number of iterations, and the condition numbers.

	$n_{\text{avg}} = 4$	$n_{\text{avg}} = 6$	$n_{\text{avg}} = 8$	$n_{\text{avg}} = 10$	$n_{\text{avg}} = 12$
CG-Uzawa:					
perm. error $e_{\kappa}^{\#}$, %	$5.4 \cdot 10^{-5}$	$4.4 \cdot 10^{-5}$	$4.3 \cdot 10^{-5}$	$3.6 \cdot 10^{-5}$	$3.4 \cdot 10^{-5}$
total comp. time, s	6.5	6.0	5.8	5.0	4.7
# iters	138	98	81	61	52
cond(S)	$4.7 \cdot 10^3$	$2.3 \cdot 10^3$	$1.3 \cdot 10^3$	$7.7 \cdot 10^2$	$5.3 \cdot 10^2$
CG-SIMPLE:					
perm. error $e_{\kappa}^{\#}$, %	$1.4 \cdot 10^{-6}$	$1.5 \cdot 10^{-6}$	$1.5 \cdot 10^{-6}$	$1.5 \cdot 10^{-6}$	$1.5 \cdot 10^{-6}$
total comp. time, s	1.4	2.4	3.5	4.6	5.7
# iters	15	22	29	35	40
cond($\hat{S}_{\text{simple}}^{-1}S$)	$3.4 \cdot 10^1$	$8.6 \cdot 10^1$	$1.6 \cdot 10^2$	$2.6 \cdot 10^2$	$3.4 \cdot 10^2$

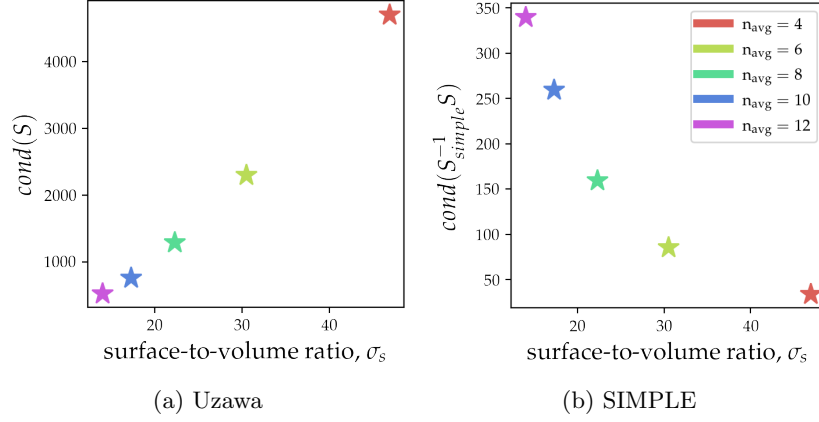
Similar observations to those made for the 3D simulations can be made from the results presented in Table 4. Again, the CG-SIMPLE algorithm requires less total computational time compared to the CG-Uzawa for low-porosity (and large surface-to-volume ratio) samples. For higher porosity, CG-Uzawa tends to show better performance. The condition number for the preconditioned Schur complement matrix (here it is computed exactly, see below) is about two orders of magnitude smaller for the SIMPLE preconditioner than for the Uzawa (identity) preconditioner in the case of low porosity. As in the 3D case, CG-SIMPLE more accurately computes permeability for low-porosity samples, indicating that it computes pressure gradient more accurately for such problems, as we discussed earlier in Section 4.1.2.

4.2.3 Correlation between the surface-to-volume ratio and the condition number of the Schur complement matrix

In Fig. 6, for the considered 2D geometries with variable channel thicknesses, we show the dependence between the surface-to-volume ratio σ_s (37) and the condition number of both the unpreconditioned and preconditioned Schur complement matrices. The main conclusion that we draw is that an increase in the surface-to-volume ratio and a decrease in porosity lead to an increase in the condition number of the Schur complement matrix. However, unlike the 3D case, for the considered here synthetic geometries the inverse dependence is clearly observed for the Schur complement matrix preconditioned with the SIMPLE.

We conjecture that for low porosity samples the condition number of the Schur complement matrix is influenced by the number of non-unit eigenvalues

Figure 6: Correlation between surface-to-volume ratio and condition number for the synthetic 2D samples with various channel thicknesses n_{avg} described in the Table 3.



in its spectrum. In the next subsection, we show that the large number of non-unit eigenvalues in the spectrum of the Schur complement matrix is directly related to low porosity and large surface-to-volume ratio.

4.2.4 Number of non-unit eigenvalues and no-slip surface area.

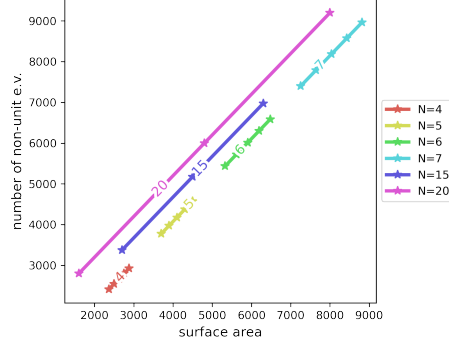
In the present section, for the class of geometries, we show the relation between surface-to-volume ratio and the number of non-unit eigenvalues of the Schur complement matrix. We consider various configurations of synthetic 2D geometries. First, we vary the number of squares N , which determines the degree of connectivity of the flow domain Ω_f . Second, for each N we vary the surface area $\mathbb{V}_{\text{surf}}^s$ defined in (38). For selected configurations, we compute the full spectrum of the Schur complement matrix S and calculate the number of eigenvalues, denoted N_{ev} , which are not equal to one, including zero eigenvalue. The results are presented in Figure 7, where we show the dependence between the surface area $\mathbb{V}_{\text{surf}}^s$ and the number of non-unit eigenvalues N_{ev} .

For the considered here class of geometries, we observe, that the following empirical formula for the number of non-unit eigenvalues holds:

$$N_{\text{ev}} = \mathbb{V}_{\text{surf}}^s + 3N^2 - 1. \quad (42)$$

In particular, the formula (42) reveals that the surface-to-volume ratio is related to the ratio of non-unit to unit eigenvalues of the Schur complement matrix, i.e., the greater is the ratio the further the Schur complement is from the identity, and the worse is the performance of the Uzawa algorithm.

Figure 7: Dependence of the number of non-unit eigenvalues of the Schur complement matrix N_{ev} on the connectivity of the flow domain and the surface area of the no-slip boundary \mathbb{V}_{surf}^s defined in (38). The number of square obstacles N in one dimension is shown by color, total N^2 obstacles.



5 Conclusions

In conclusion, the article presents a comparative study of the CG-SIMPLE and CG-Uzawa algorithms for samples with low porosity. The results show that the CG-SIMPLE algorithm applied to solve Stokes problem for low porosity 3D rock samples provides significantly lower condition numbers of the Schur complement matrix and ensures robust convergence to high accuracy both in solving the Schur complement problem and in computing the permeability. The latter indicates that the pressure gradient is more accurately computed in this case. This behavior is further explained through a systematic study of synthetic 2D geometries. We demonstrate that the number of non-unit eigenvalues of the Schur complement matrix is determined by the surface area of the boundary where the no-slip conditions are posed, and the connectivity of the flow domain. Moreover, we show that an increase in the surface-to-volume ratio leads to an increase in the condition number of the Schur complement matrix. However, the inverse correlation holds for the Schur complement matrix preconditioned with the SIMPLE. These findings provide important insights into the behavior of the solvers for the Schur complement matrix and suggest effectiveness of the SIMPLE preconditioner for solving the Stokes problem in tight geometries.

Acknowledgements

Ivan Oseledets was supported by Alexander von Humboldt Research Award. Oleg Iliev was supported by BMBF under grant 05M20AMD ML-MORE.

References

- [1] Owe Axelsson and János Karátson. Krylov improvements of the uzawa method for stokes type operator matrices. *Numerische Mathematik*, 148(3):611–631, 2021.
- [2] Owe Axelsson and Maya Neytcheva. Preconditioning methods for linear systems arising in constrained optimization problems. *Numerical linear algebra with applications*, 10(1-2):3–31, 2003.
- [3] Owe Axelsson and Maya Neytcheva. Eigenvalue estimates for preconditioned saddle point matrices. *Numerical Linear Algebra with Applications*, 13(4):339–360, 2006.
- [4] Michele Benzi, Gene H Golub, and Jörg Liesen. Numerical solution of saddle point problems. *Acta numerica*, 14:1–137, 2005.
- [5] James H Bramble and Joseph E Pasciak. Iterative techniques for time dependent stokes problems. *Computers & Mathematics with Applications*, 33(1-2):13–30, 1997.
- [6] James H Bramble, Joseph E Pasciak, and Apostol T Vassilev. Analysis of the inexact uzawa algorithm for saddle point problems. *SIAM Journal on Numerical Analysis*, 34(3):1072–1092, 1997.
- [7] Howard Elman, Victoria E Howle, John Shadid, Robert Shuttleworth, and Ray Tuminaro. A taxonomy and comparison of parallel block multi-level preconditioners for the incompressible navier–stokes equations. *Journal of Computational Physics*, 227(3):1790–1808, 2008.
- [8] Howard C Elman and Gene H Golub. Inexact and preconditioned uzawa algorithms for saddle point problems. *SIAM Journal on Numerical Analysis*, 31(6):1645–1661, 1994.
- [9] Michel Fortin and Roland Glowinski. *Augmented Lagrangian methods: applications to the numerical solution of boundary-value problems*. Elsevier, 2000.
- [10] Gene H Golub and Michael L Overton. The convergence of inexact chebyshev and richardson iterative methods for solving linear systems. *Numerische Mathematik*, 53(5):571–593, 1988.
- [11] Michael Griebel, Thomas Dornseifer, and Tilman Neunhoffer. *Numerical simulation in fluid dynamics: a practical introduction*. SIAM, 1998.
- [12] Francis H Harlow and J Eddie Welch. Numerical calculation of time-dependent viscous incompressible flow of fluid with free surface. *The physics of fluids*, 8(12):2182–2189, 1965.

- [13] James M Hyman and Mikhail Shashkov. Adjoint operators for the natural discretizations of the divergence, gradient and curl on logically rectangular grids. *Applied Numerical Mathematics*, 25(4):413–442, 1997.
- [14] Vyacheslav Ivanovich Lebedev. On the grid method for a system of partial differential equations (in russian). *Proceedings of the Russian Academy of Sciences. Mathematical series*, 22(5):717–734, 1958.
- [15] Andreas Meier, Eberhard Bänsch, and Florian Frank. Schur preconditioning of the stokes equations in channel-dominated domains. *Computer Methods in Applied Mechanics and Engineering*, 398:115264, 2022.
- [16] Yvan Notay. A new analysis of block preconditioners for saddle point problems. *SIAM journal on Matrix Analysis and Applications*, 35(1):143–173, 2014.
- [17] Yvan Notay. Convergence of some iterative methods for symmetric saddle point linear systems. *SIAM Journal on Matrix Analysis and Applications*, 40(1):122–146, 2019.
- [18] Denis Orlov, Mohammad Ebadi, Ekaterina Muravleva, Denis Volkhonskiy, Andrei Erofeev, Evgeny Savenkov, Vladislav Balashov, Boris Belozerov, Vladislav Krutko, Ivan Yakimchuk, et al. Different methods of permeability calculation in digital twins of tight sandstones. *Journal of Natural Gas Science and Engineering*, 87:103750, 2021.
- [19] Suhas V Patankar and D Brian Spalding. A calculation procedure for heat, mass and momentum transfer in three-dimensional parabolic flows. In *Numerical prediction of flow, heat transfer, turbulence and combustion*, pages 54–73. Elsevier, 1983.
- [20] Vladislav Pimanov, Vladislav Lukoshkin, Pavel Toktaliev, Oleg Iliev, Ekaterina Muravleva, Denis Orlov, Vladislav Krutko, Alexander Avdonin, Konrad Steiner, and Dmitry Koroteev. On a workflow for efficient computation of the permeability of tight sandstones. *arXiv preprint arXiv:2203.11782*, 2022.
- [21] John W Ruge and Klaus Stüben. Algebraic multigrid. In *Multigrid methods*, pages 73–130. SIAM, 1987.
- [22] Mihail Shashkov. *Support operator methods and numerical modeling hydrodynamic flows in the case of strong deformations (in Russian)*. PhD thesis, Moscow State University, Faculty of Computational Mathematics and Cybernetics, 1989.
- [23] Stefan Turek. *Efficient Solvers for Incompressible Flow Problems: An Algorithmic and Computational Approaches*, volume 6. Springer Science & Business Media, 1999.

- [24] Rudiger Verfurth. A combined conjugate gradient-multi-grid algorithm for the numerical solution of the stokes problem. *IMA Journal of Numerical Analysis*, 4(4):441–455, 1984.
- [25] Alexey Voronin, Yunhui He, Scott MacLachlan, Luke N Olson, and Raymond Tuminaro. Low-order preconditioning of the stokes equations. *Numerical Linear Algebra with Applications*, 29(3):e2426, 2022.
- [26] A Wiegmann. Computation of the permeability of porous materials from their microstructure by fff-stokes. *Berichte des Fraunhofer ITWM*, 2007 (129), 2007.
- [27] Ulrike Meier Yang et al. Boomeramg: a parallel algebraic multigrid solver and preconditioner. *Applied Numerical Mathematics*, 41(1):155–177, 2002.